

1 **Impact of restriction of the Atlantic-Mediterranean gateway on the Mediterranean**
2 **Outflow Water and eastern Atlantic circulation during the Messinian**

3

4 J. N. Pérez-Asensio,¹ J. Aguirre,¹ G. Schmiedl,² and J. Civis³

5

6 ¹Departamento de Estratigrafía y Paleontología, Facultad de Ciencias, Avenida
7 Fuentenueva s.n., Universidad de Granada, 18002 Granada, Spain. (jnoel@ugr.es;
8 jaguirre@ugr.es).

9 ²Department of Geosciences, University of Hamburg, 20146 Hamburg, Germany.
10 (gerhard.schmiedl@uni-hamburg.de).

11 ³Departamento de Geología, Universidad de Salamanca, 37008 Salamanca, Spain.
12 (civis@usal.es).

13

14 Corresponding author: J. N. Pérez-Asensio, Departamento de Estratigrafía y
15 Paleontología, Facultad de Ciencias, Avenida Fuentenueva s.n., Universidad de
16 Granada, 18002 Granada, Spain. (jnoel@ugr.es).

17

18 **Abstract**

19 Messinian foraminiferal stable oxygen and carbon isotopes of the Montemayor-1
20 core (Guadalquivir Basin, SW Spain) have been investigated. This record is exceptional
21 to study the Mediterranean Outflow Water (MOW) impact on the Atlantic meridional
22 overturning circulation (AMOC) and global climate during the Messinian because the
23 core is near the Guadalorce Corridor, the last Betic gateway to be closed during the
24 early Messinian. Our results allow dating accurately its closure at 6.18 Ma. Constant
25 benthic $\delta^{18}\text{O}$ values, high difference between benthic and planktonic $\delta^{18}\text{O}$, and low

26 sedimentation rates before 6.18 Ma indicate the presence of a two-layer water column,
27 with bottom winnowing due to an enhanced Mediterranean outflow current. The
28 enhanced contribution of dense MOW to the North Atlantic Ocean likely fostered the
29 formation of North Atlantic deep water (NADW). After 6.18 Ma, benthic $\delta^{18}\text{O}$ values
30 parallel that of the global glacioeustatic curve, the difference between benthic and
31 planktonic $\delta^{18}\text{O}$ is low, and sedimentation rates considerably increased. This indicates a
32 good vertical mixing of the water column, interruption of the MOW, and a dominant
33 glacioeustatic control on the isotopic signatures. According to the role of MOW in the
34 modern Atlantic thermohaline circulation, the reduction of the MOW after the closure
35 of the Guadalhorce Corridor might have resulted in a decreased NADW formation rate
36 between 6.0 and 5.5 Ma weakening the AMOC and promoting northern hemisphere
37 cooling. After the Gibraltar Strait opening, the restoration of the MOW and related salt
38 export from the Mediterranean could have promoted an enhanced NADW formation.

39

40 **1. Introduction**

41 At present, the Mediterranean connects with the Atlantic by the Strait of
42 Gibraltar. The water mass exchange throughout the Strait of Gibraltar is characterized
43 by an anti-estuarine circulation pattern (Figure 1a) [*Wüst*, 1961]. This anti-estuarine
44 circulation pattern was definitively established after the opening of the Strait of
45 Gibraltar [*Nelson*, 1990], although it has been suggested that the movements of water
46 masses reversed to estuarine-type circulation during the early Pleistocene [*Huang and*
47 *Stanley*, 1972]. Lower salinity surface waters from the North Atlantic flow superficially
48 eastwards into the Mediterranean (Figure 1a). On the other hand, strong evaporation and
49 production of dense, saline intermediate and deep-water in the eastern Mediterranean
50 forces a high-velocity density driven bottom current westwards as MOW through the

51 Strait of Gibraltar. This mass of water is mainly fed by the Levantine Intermediate
52 Water (LIW) [Bryden and Stommel, 1984], formed by convection in the Eastern
53 Mediterranean [Marshall and Schott, 1999; Hernández-Molina et al., 2011], and in
54 lesser extent by the Western Mediterranean Deep Water (WMDW), which is formed in
55 the Gulf of Lion during cold and windy winters [MEDOC Group, 1970; Bryden and
56 Stommel, 1984; Lacombe et al., 1985]. Today, the LIW contributes to 2/3 of the MOW
57 while WMDW only represents 1/3 of the MOW [Millot, 1999]. Therefore, the LIW
58 might be more important in controlling the MOW than WMDW. The MOW is
59 characterized by higher $\delta^{13}\text{C}$ and $\delta^{18}\text{O}$ than the Atlantic waters [Vergnaud-Grazzini,
60 1983; Sierro et al., 2005].

61 The outflow of the MOW into the Eastern Atlantic has a significant effect on the
62 Atlantic oceanic circulation as well as on the global climate. The dense MOW mixes
63 with the North Atlantic intermediate waters forming a high salinity tongue (Figure 1b)
64 that contributes to the momentum of the Atlantic meridional overturning circulation
65 (AMOC) [Reid, 1979; Rahmstorf, 1998; Bigg and Wadley, 2001; Bigg et al., 2003]. In
66 turn, the AMOC is the driving force for the Atlantic Ocean circulation, and even the
67 global thermohaline circulation [Bethoux et al., 1999]. Global thermohaline circulation
68 affects the global radiation budget and global carbon cycling and can thus produce
69 major climate changes [Brown et al., 1989; Bigg et al., 2003; Murphy et al., 2009].
70 Therefore, a reduction or interruption of the MOW could have a critical impact both on
71 the AMOC and on the global circulation, as well as on the global climate. Without the
72 contribution of the saline MOW, the formation of dense water, which triggers the
73 AMOC, would have most likely not taken place steadily in the North Atlantic
74 [Rahmstorf, 1998; Bethoux et al., 1999].

75 The impact of the MOW on the Atlantic Ocean circulation during the Pliocene,
76 Pleistocene, and Holocene, has been comprehensively studied [*Loubere, 1987; Nelson*
77 *et al., 1993; Schönfeld, 1997; Maldonado and Nelson, 1999; Schönfeld and Zahn, 2000;*
78 *Rogerson et al., 2005; Hernández-Molina et al., 2006, 2011; Llave et al., 2006, 2011;*
79 *Toucanne et al., 2007; Khélifi et al., 2009; Rogerson et al., 2010, 2011, 2012; Stumpf et*
80 *al., 2010; van Rooij et al., 2010; Estrada et al., 2011*]. These studies show an Upper
81 North Atlantic Deep Water (UNADW) formation produced by an enhanced MOW flow
82 related to an increased Mediterranean deep-water formation and enhanced aridity in the
83 Mediterranean region. Furthermore, the supply of salt by the MOW into the
84 intermediate North Atlantic waters favors the resumption of the AMOC during
85 interglacials [*Rogerson et al., 2006, 2012; Voelker et al., 2006*].

86 All these studies have analyzed the history and impact of the MOW on the
87 Atlantic circulation after the end of Messinian salinity crisis (MSC), when the Atlantic-
88 Mediterranean connections were reestablished through the Strait of Gibraltar. However,
89 little is known about the impact of the MOW during the Messinian, when the
90 connections were through the Betic and Rifian Corridors [*van der Laan et al., 2012*] or
91 after the cessation of the MOW due to the closure of these corridors. *Keigwin et al.*
92 [1987] questioned that the MSC had any effect on the deep circulation in the North
93 Atlantic. On the contrary, *Zhang and Scott [1996]* reported the presence of the MOW at
94 the northeastern Atlantic Ocean, at least reaching 50°N of latitude, during the
95 Messinian. Moreover, Pb and Nd isotopic studies also pointed out to the influence of the
96 MOW in the NE Atlantic during the Messinian [*Abouchami et al., 1999*]. Apart from
97 these works deciphering the influence of the MOW in the distant Atlantic, no study has
98 focused on the areas close to the Atlantic-Mediterranean connections in the Betics.

99 It has been largely substantiated that the restriction of the Atlantic-
100 Mediterranean connections played a major role in the onset of the MSC [e.g. *Esteban et*
101 *al.*, 1996; *Riding et al.*, 1998; *Krijgsman et al.*, 1999a, 1999b; *Martín et al.*, 2001;
102 *Braga et al.*, 2006]. The Betic Corridors together with their southern counterparts, the
103 Rifian Corridors (NW Morocco), were the main gateways connecting the Atlantic and
104 Mediterranean until their closure [*Benson et al.*, 1991; *Esteban et al.*, 1996; *Martín et*
105 *al.*, 2001, 2009; *Betzler et al.*, 2006].

106 The Guadalquivir Basin, located in the south of the Iberian Peninsula, represents
107 the Atlantic side of the Betic Corridors that extended through southern Spain during the
108 early late Miocene [*Benson et al.*, 1991; *Martín et al.*, 2001, 2009; *Braga et al.*, 2002].
109 The last active Betic gateway was the Guadalhorce Corridor, which controlled the
110 Messinian pre-evaporitic circulation in the western Mediterranean, and allowed the
111 MOW to enter the Atlantic Ocean [*Martín et al.*, 2001]. The Guadalhorce Corridor was
112 a NW-SE trending strait with an estimated maximum width of 5 km and maximum
113 water depth of 120 m [*Martín et al.*, 2001]. The corridor was filled by sediment
114 displaying huge unidirectional sedimentary structures indicating Mediterranean waters
115 flowing out into the Atlantic at estimated current velocities of about 1.0-1.5 m/s [*Martín*
116 *et al.*, 2001]. This water mass circulation is consistent with the siphon model of *Benson*
117 *et al.* [1991] stating that prior to the closure of the Betic Corridors, the water exchange
118 between the Mediterranean and the Atlantic during the Messinian was characterized by
119 Atlantic inflow through the Rifian Corridors and MOW through the Guadalhorce
120 Corridor [*Benson et al.*, 1991; *Martín et al.*, 2001]. After the closure of the Guadalhorce
121 Corridor in the early Messinian [*Martín et al.*, 2001], MOW was interrupted and
122 circulation was restricted to the Rifian Corridors [*Esteban et al.*, 1996]. Later the
123 closure of the Rifian Corridors in the late Messinian [*Krijgsman et al.*, 1999a] caused

124 the isolation of the Mediterranean Sea and, consequently, a hydrographical deficit that
125 triggered the onset of the MSC with deposition of extensive evaporites in the central
126 and deeper parts of the Mediterranean [*Hsü et al.*, 1973, 1977].

127 In this study, we examine the impact of the MOW during the Messinian close to
128 the Betic corridors. We analyze foraminiferal stable O and C isotope composition in the
129 Montemayor-1 core (SW Spain) (Figure 2). The core site is located close to the
130 Guadalhorce Corridor, the last Betic corridor to be closed [*Martín et al.*, 2001, 2009],
131 and shows a continuous Messinian record accurately dated by magnetobiostratigraphic
132 methods [*Larrasoña et al.*, 2008]. The Guadalquivir Basin was well connected with
133 the Atlantic Ocean during the MSC, so there was neither desiccation nor evaporite
134 deposition. Furthermore, according to the siphon model of *Benson et al.* [1991],
135 Mediterranean outflow took place only throughout the Betic Corridors. Therefore, the
136 location of the core is exceptional to study the effect of the MOW on the eastern
137 Atlantic Ocean circulation during the Messinian, as well as its possible impact on global
138 climate changes.

139 The main aims of this study are: 1) to assess the impact of the MOW on the
140 AMOC during the Messinian; and 2) to precisely date the closure of the Guadalhorce
141 Corridor.

142

143 **2. Geological Setting**

144 The study area is located in the westernmost part of the northwestern edge of the
145 lower Guadalquivir Basin (SW Spain) (Figure 2). This is an ENE-WSW elongated
146 Atlantic Neogene foreland basin [*Sanz de Galdeano and Vera*, 1992; *Vera*, 2000; *Braga*
147 *et al.*, 2002] with a sedimentary infilling consisting of marine and continental sediments
148 ranging from the early Tortonian to the late Pliocene [*Aguirre*, 1992, 1995; *Aguirre et*

149 *al.*, 1993, 1995; *Riaza and Martínez del Olmo*, 1996; *Sierro et al.*, 1996; *Braga et al.*,
150 2002; *González-Delgado et al.*, 2004; *Martín et al.*, 2009].

151 The Guadalquivir foreland basin was formed as a consequence of the Betic
152 Cordillera compressional overthrusting during the early-middle Miocene [*Sanz de*
153 *Galdeano and Vera*, 1992; *Riaza and Martínez del Olmo*, 1996; *Sanz de Galdeano and*
154 *Rodríguez-Fernández*, 1996; *Martín et al.*, 2009; *Braga et al.*, 2010]. During the
155 Serravallian, the Atlantic-Mediterranean connection started to be restricted in the
156 northeastern edge of the Guadalquivir Basin, in the Prebetic Domain of the Betic
157 Cordillera [*Aguirre et al.*, 2007; *Martín et al.*, 2009; *Braga et al.*, 2010]. The
158 progressive tectonic uplifting of the Betic mountain chain led to a progressive closure of
159 this seaway, originating the so-called North Betic Strait during the latest middle
160 Miocene-earliest late Miocene (topmost Serravallian-earliest Tortonian) [*Aguirre et al.*,
161 2007; *Martín et al.*, 2009; *Braga et al.*, 2010]. The final closure of the North Betic Strait
162 took place during the early Tortonian [*Sierro et al.*, 1996; *Martín et al.*, 2009; *Braga et*
163 *al.*, 2010] and the Guadalquivir Basin was established as a wide, marine embayment
164 only opened to the Atlantic Ocean [*Martín et al.*, 2009].

165 After the cessation of the North Betic Strait, other Betic gateways connected the
166 Atlantic and the Mediterranean through the Guadalquivir Basin. They were
167 progressively closed during the late Miocene. In the late Tortonian, the Dehesas de
168 Guadix Corridor and the Granada Basin were the main Atlantic-Mediterranean
169 connections [*Esteban et al.*, 1996; *Braga et al.*, 2003; *Betzler et al.*, 2006; *Martín et al.*,
170 2009]. After their closure, the Guadalhorce Corridor was the only connection during the
171 earliest Messinian [*Martín et al.*, 2001]. This last Betic Corridor became closed in the
172 early Messinian [*Martín et al.*, 2001]. Since its closure, the Rifian Corridors were the
173 unique Atlantic-Mediterranean gateways [*Esteban et al.*, 1996].

174

175 **3. Material and Methods**

176 **3.1. Montemayor-1 Core**

177 The studied material is the Montemayor-1 core, a 260 m long core that has been
178 drilled in the northwestern margin of the lower Guadalquivir Basin close to Moguer
179 (SW Spain) (Figures 2 and 3). This core includes marine sediments that can be divided
180 into four lithostratigraphic units [see a detail description in *Pérez-Asensio et al.*, 2012]
181 (Figure 3): the Niebla Formation (Tortonian), the Arcillas de Gibraleón Formation
182 (latest Tortonian-Messinian), the Arenas de Huelva Formation (early Pliocene), and the
183 Arenas de Bonares Formation (late Pliocene-Pleistocene).

184 In this study, we analyzed an interval of 70 m, from 240 to 170 m (from 6.67 Ma
185 to 5.7 Ma according to the age model. See below), including Messinian sediments from
186 the Arcillas de Gibraleón Formation (Figure 3). In this interval, a total of 132 samples
187 were collected with a sampling interval of 0.5 m. Samples were wet sieved over a 63
188 μm mesh and dried out in an oven at 40 °C. A representative split was dry-sieved over a
189 125 μm mesh to estimate the planktonic/benthic ratio (P/B ratio henceforth), calculated
190 as $[P/(P+B)]$ as a proxy for relative sea-level change.

191 **3.2. Stable Isotope Analyses**

192 Stable isotope analyses ($\delta^{18}\text{O}$ and $\delta^{13}\text{C}$) were performed on 10 individuals of
193 *Cibicidoides pachydermus* for benthic foraminifera and 20 individuals of *Globigerina*
194 *bulloides* for planktonic foraminifera separated from the size fraction $>125 \mu\text{m}$.
195 Foraminiferal shells were ultrasonically cleaned, and washed with distilled water prior
196 to the analyses. The isotopic analyses were performed on a Finnigan MAT 251 mass
197 spectrometer connected to a Kiel I (prototype) preparation device for carbonates at the
198 Leibniz-Laboratory for Radiometric Dating and Isotope Research, Kiel, Germany.

199 Results are given in δ -notation in per mil, and are reported on the Vienna Pee Dee
200 belemnite (VPDB) scale. The VPDB scale is defined by a certain value of the National
201 Bureau of Standards (NBS) carbonate standard NBS-19. On the basis of the
202 international and lab-internal standard material, the analytical reproducibility is $< \pm 0.05$
203 ‰ for $\delta^{13}\text{C}$, and $< \pm 0.07$ ‰ for $\delta^{18}\text{O}$.

204 **3.3. Spectral Analyses**

205 Spectral analysis was performed in order to identify the nature and significance
206 of periodic changes in the benthic $\delta^{18}\text{O}$ record. The analysis was carried out in the time
207 domain using the software PAST [*Hammer et al.*, 2001] and the REDFIT procedure of
208 *Schulz and Mudelsee* [2002]. This procedure allows assessing the spectral analysis with
209 unevenly spaced samples. Spectral peaks over the 95% confidence interval (CI) were
210 considered significant.

211

212 **4. Age Model**

213 The age model of the Montemayor-1 core was established using a combination
214 of paleomagnetism, biostratigraphy, and stable oxygen isotope stratigraphy (Figure 3).
215 The reversed chron C3r is almost continuously recorded since a discontinuity is
216 detected close to the boundary between chrons C3r and C3n, which prevent us from
217 using this magnetostratigraphic reversal boundary as a chronological datum in the upper
218 part of the core [*Pérez-Asensio et al.*, 2012].

219 To complete the age model above the normal magnetic chron C3An.1n, we have
220 used the glacial stage TG 22 as a tie point, which was astronomically calibrated at 5.79
221 Ma [*Krijgsman et al.*, 2004]. We identified this glacial stage by means of stable oxygen
222 isotope stratigraphy (Figure 4). The benthic oxygen isotope record shows two distinctly
223 pronounced “paired” glacial peak stages that we identify as the glacial stages TG 20 and

224 TG 22 (Figure 4) according to the nomenclature established by *Shackleton et al.* [1995].
225 These two stages are easily identifiable because they are the most pronounced “paired”
226 glacial peaks at the end of a progressively increasing trend in the $\delta^{18}\text{O}$ record along the
227 chron C3r (Figure 4). Both the isotopic trend and the two “paired” glacial maxima are
228 evident and have been observed in other cores at global scale including the Pacific
229 Ocean [*Shackleton et al.*, 1995], the Atlantic Ocean [*Hodell et al.*, 2001; *Vidal et al.*,
230 2002], as well as in sediments from the Rifian Corridors [*Hodell et al.*, 1994].

231 Using the TG 22 as a tie point in the chronological framework, the estimated age
232 for the TG 20 based on the reconstructed sedimentation rate (14.8 cm/kyr) is 5.75 Ma
233 (Figures 3 and 5). This age estimation is coincident with the age estimated by
234 *Krijgsman et al.* [2004] using astronomical tuning.

235 Further to the TG 20 and TG 22, we have identified the rest of the glacial stages
236 following the nomenclature of *Shackleton et al.* [1995]. These authors found that the
237 benthic O isotope record was controlled by 41-kyr cycles related to orbital obliquity.
238 *Hodell et al.* [1994] also showed that the benthic isotope record from the Salé
239 Briqueterie core at the Rifian Corridors reflects obliquity induced changes. The benthic
240 oxygen isotope record from the Montemayor-1 core is also mainly controlled by 41-kyr
241 cycles related to orbital obliquity (Figure 6).

242 Since the TG glacial stages of *Shackleton et al.* [1995] were related to obliquity,
243 we use the same methodology to identify the rest of the TG stages in the chron C3r.
244 Further, in order to confirm the reliability of the identification of TG 20 and TG 22 in
245 the Montemayor-1 core, we plot the benthic isotope record versus age (Ma), including
246 the TG 22 datum (5.79 Ma), and counted obliquity cycles backwards (Figure 5).
247 Comparing the benthic oxygen isotope record from the Montemayor-1 core with its
248 obliquity component (Figure 5) we identified up to stage TG 32 for chron C3r.

249 However, *Hodell et al.* [1994] and *van der Laan et al.* [2005] recognized one extra
250 obliquity cycle, up to TG 34 stage. The discrepancy in just one obliquity cycle (1 glacial
251 stage and 1 interglacial stage) can be due to the fact that *Hodell et al.* [1994] identified
252 glacial stages versus depth instead of time. This could result in counting cycles of
253 different periodicities. On the other hand, *van der Laan et al.* [2005], considered the
254 glacial stage TG 30, which is a precession-related signal, at the same level of the rest of
255 the obliquity-related cycles.

256

257 **5. Results**

258 The benthic oxygen isotope record shows stable values around 1‰ before 6.35
259 Ma, and then it decreases reaching a minimum of -0.93‰ at 6.18 Ma (Figure 7). After
260 6.18 Ma, it exhibits fluctuations with a trend towards heavier values reaching the
261 maximum values at 5.79 Ma (TG 22), and then it decreases towards lighter values
262 (Figure 7). The benthic stable O isotope curves of the Montemayor-1 core and site 1085
263 [*Vidal et al.*, 2002] reveal different trends for the time interval before 6.18 Ma (Figure
264 5). On the contrary, both curves show a parallel trend with similar fluctuations after
265 6.18 Ma. In this interval, heavy values of $\delta^{18}\text{O}$ from the Montemayor-1 core can be
266 easily matched with glacial peaks from site 1085 (Figure 5).

267 The planktonic oxygen isotope record exhibits a fluctuating trend with values \leq
268 0‰ before 6.18 Ma and values > 0 ‰ after this age (Figure 7). Both the benthic and
269 planktonic O isotopic curves follow different trends before 6.18 Ma. After 6.18 Ma, the
270 planktonic O isotopic curve parallels that of the benthic one except for some low values
271 around 5.79 Ma (Figure 7). The similar trend of both records is confirmed by a
272 statistically significant positive correlation ($\rho = 0.415$). The $\Delta\delta^{18}\text{O}_{\text{benthic-planktonic}}$ ($\Delta\delta^{18}\text{O}_{\text{b-}}$
273 p) curve reflects these differences before and after 6.18 Ma between the benthic and

274 planktonic O isotope values, being higher before 6.18 Ma (Figure 7). The difference
275 reaches average values close to 0 at around 6.2 Ma (Figure 7).

276 The planktonic carbon isotope record exhibits significant fluctuations with
277 average values around -0.8‰ before 6.18 Ma (Figure 7). After 6.18 Ma, the $\delta^{13}\text{C}$
278 decreases reaching its lowest values from 6.05 to 5.85 Ma. Then, it drastically increases
279 from average values of -1‰ to 0‰ at 5.85 Ma, and remains with relatively high average
280 values around 0 until 5.77 Ma. At this age, another carbon shift took place recovering
281 average values of -1‰ (Figure 7). The benthic carbon isotope record shows fluctuations
282 with average values around 0.4‰ before 6.18 Ma. After 6.18 Ma, the $\delta^{13}\text{C}$ decreases
283 reaching its lowest values from 6 to 5.9 Ma. Finally, it increases and remains with
284 relatively high values around 0.4‰ from 5.9 to 5.7 Ma (Figure 7).

285

286 **6. Discussion**

287 **6.1. Identification of the MOW in the northeastern Atlantic and age of the closure** 288 **of the Guadalhorce Corridor**

289 **6.1.1. MOW presence before 6.18 Ma**

290 The benthic O isotopic values from the Montemayor-1 core depart from the
291 fluctuating global trend, based on *Vidal et al.* [2002], from the base of the studied
292 interval to 6.18 Ma (Figure 5). The presence of a dense, i.e. highly saline, bottom water
293 mass affecting the study area might account for the observed deviation towards heavier
294 values in the O isotope record.

295 The Montemayor-1 core site is located adjacent to the Guadalhorce Corridor, the
296 last Atlantic-Mediterranean gateway providing a connection between the Mediterranean
297 and Atlantic oceans through the Betic Cordillera prior to the onset of the MSC (Figure
298 8a). Based on the vicinity of the core site to this gateway it appears most likely that the

299 benthic habitats of the study area were bathed by the highly saline MOW prior to 6.18
300 Ma (Figure 8a).

301 In the Montemayor-1 core, benthic O values remain approximately constant at
302 around 1‰ before 6.35 Ma. This suggests a more or less constant MOW flux as
303 indicated by the scarcity of reactivation surfaces in the sedimentary structures of the
304 Guadalhorce Corridor [Martín *et al.*, 2001]. The benthic stable O isotope values of 1‰
305 reflect the density of the MOW that is the product of mixing between the exported
306 Mediterranean water and the ambient Atlantic water. This value is in the range of recent
307 benthic stable O isotope values of the upper core of the MOW, which ranges between 1
308 and 2‰ [Rogerson *et al.*, 2011]. Before 6.35 Ma the exchange through the Guadalhorce
309 Corridor is expected to be maximal because of the increased density between the MOW
310 and Atlantic surface waters ($\Delta\delta^{18}\text{O}_{\text{b-p}}$) and the high sea-level indicated by the P/B ratios
311 (Figure 7). The benthic C isotope record could partially reflect MOW activity. Using the
312 modern analogue, high values of benthic $\delta^{13}\text{C}$ are associated to MOW because of the
313 low residence time of this water mass [Vergnaud-Grazzini, 1983; Schönfeld and Zahn,
314 2000; Raddatz *et al.*, 2011; Rogerson *et al.*, 2011]. Thus, relatively high benthic C
315 isotopic values around 6.4-6.5 Ma might be the result of increased MOW presence
316 (Figure 7).

317 The presence of the MOW before 6.18 Ma is also supported by the
318 paleobathymetry of the study area during this period. At the present-day, the MOW
319 entering the Atlantic flows along the western Iberian continental slope between 400 and
320 1,500 m water depth [Schönfeld and Zahn, 2000; Llave *et al.*, 2006]. In the study area,
321 the presence of R-mode *Anomalinoides flinti* assemblage and *Planulina ariminensis*
322 before 6.18 Ma (below 227.5 m core depth in Pérez-Asensio *et al.*, 2012) indicates that

323 the current flowed along the middle and upper slope [*Pérez-Asensio et al.*, 2012]. This
324 is within the depth range of MOW flow at the present-day.

325 A comparison between benthic and planktonic O isotopic records from the
326 Montemayor-1 core offers another indication of the MOW presence before 6.18 Ma.
327 The decoupling and high difference between the benthic and planktonic O isotopic
328 signals before 6.18 Ma (Figure 7) are indicative of a two-layer water column with the
329 presence of MOW at the sea floor. Moreover, the lowest sedimentation rates are
330 estimated before 6.18 Ma (Figure 3). Thus, winnowing by the MOW might most likely
331 account for this result.

332 **6.1.2. Response of the MOW plume to the restriction of the Guadalhorce Corridor** 333 **(6.35 to 6.18 Ma)**

334 Between 6.35 and 6.18 Ma, the benthic O isotopic record underwent a
335 significant negative excursion of about 2‰, from 1‰ to a minimum of -0.93‰ (Figures
336 5 and 7). This noteworthy isotopic shift suggests a MOW product with a lighter O
337 isotopic signature. The ambient Atlantic water has a lower density than the MOW
338 [*Price and O'Neil-Baringer*, 1994]. Hence, the local minimum in the benthic $\delta^{18}\text{O}$ from
339 6.35 to 6.18 Ma could be explained by a higher proportion of the lighter ambient
340 Atlantic water in the final MOW product as occurs at present-day outside the upper core
341 of the MOW plume [*Rogerson et al.*, 2011]. In addition, this fact could reflect a gradual
342 reduction in the exchange through the Guadalhorce Corridor as it is indicated by the
343 reduction of density between the MOW and the Atlantic surface waters ($\Delta\delta^{18}\text{O}_{\text{b-p}}$) and
344 relatively low sea-level (Figure 7). The reduced exchange from 6.35 to 6.18 Ma is also
345 reflected by the decrease in the benthic C isotopes (Figure 7). Similarly, the diminished
346 outflow of Mediterranean waters in the Rifian Corridors is indicated by a negative
347 excursion in the planktonic C isotopes at 6.0 Ma [*van der Laan et al.*, 2012].

348 Alternatively, the local minimum in the benthic $\delta^{18}\text{O}$ might reflect the isotopic
349 signature of less dense Atlantic waters. Increased salinity of Mediterranean source
350 waters due to the restriction of the Guadalhorce Corridor could produce a denser MOW
351 that mixes faster with ambient Atlantic waters reducing its density and consequently
352 shoaling on the slope [Rogerson *et al.*, 2012]. Therefore, the location of the
353 Montemayor-1 core would be beneath the MOW between 6.35 and 6.18 Ma. Our data
354 from the Montemayor-1 core do not allow us to rule out any of these two alternative
355 explanations.

356 **6.1.3. Cessation of the MOW at 6.18 Ma**

357 After 6.18 Ma, the benthic $\delta^{18}\text{O}$ parallels that of the global benthic O record,
358 with main glacial stages easily distinguishable in both records (Figure 5). Therefore,
359 benthic O isotopic values at the study area were primarily controlled by global
360 glacioeustatic fluctuations. Most likely, the striking change in the $\delta^{18}\text{O}$ record at 6.18
361 Ma can be linked with the cessation of the dense MOW influence in the study area
362 (Figure 8b).

363 A comparison between benthic and planktonic O isotopic records from the
364 Montemayor-1 core also supports the interruption of the MOW after 6.18 Ma. Benthic
365 and planktonic O isotopic values covary after 6.18 Ma indicating enhanced vertical
366 mixing and absence of MOW. This is also supported by low $\Delta\delta^{18}\text{O}_{\text{b-p}}$ and positive
367 statistical correlation between benthic and planktonic O isotopic values ($\rho = 0.415$)
368 (Figure 7). The covariation and the decreasing difference between planktonic and
369 benthic O isotopes might have also been favored by the shallowing-upward trend that
370 reduces the difference between benthic and planktonic isotopic values.

371 Moreover, sedimentation rate could be affected by the interruption of the MOW
372 at 6.18 Ma. After this date, sedimentation rates drastically increases from 6.3 to 14.8

373 cm/kyr (Figure 3) likely due to the interruption of the MOW and the resulting
374 progradation of depositional systems along the axis of the Guadalquivir Basin [*Sierro et*
375 *al.*, 1996] (Figure 8b).

376 The closure of this corridor at 6.18 Ma caused the final interruption of MOW.
377 The observed age for the end of this Betic gateway is consistent with planktonic
378 foraminifera recorded in the sediments filling the Guadalhorce Corridor that indicate
379 that the strait was open at least from 7.2 to 6.3 Ma [*Martín et al.*, 2001]. Further, it is
380 also coincident with the first land mammal exchange between Africa and the Iberian
381 Peninsula prior to the MSC taking place at 6.1 Ma [*Garcés et al.*, 1998]. Therefore,
382 according to our data, the closure of the Guadalhorce Corridor (6.18 Ma) predates by
383 about 220-kyr the onset of the MSC, dated at 5.96 ± 0.02 Ma by *Krijgsman et al.*
384 [1999b].

385

386 **6.2. Impact of the MOW on the eastern North Atlantic Ocean circulation**

387 The MOW is essential to maintain the meridional overturning circulation
388 (AMOC) because it increases the North Atlantic density gradient and can restart the
389 AMOC after its collapse [*Rogerson et al.*, 2012]. It appears likely that any fluctuation of
390 the MOW can alter the AMOC. During the Messinian period, the increase of the
391 NADW presence in the South Atlantic Ocean between 6.6 and 6.0 Ma [*Billups, 2002*]
392 suggests an enhanced NADW formation due to the suspected salinity increase of the
393 MOW before the closure of the Atlantic-Mediterranean gateways. During this interval,
394 MOW affected our study area before the closure of the Guadalhorce Corridor at 6.18
395 Ma (Figures 5 and 7). It has to be mentioned however, that the increase in NADW flow
396 in the South Atlantic Ocean could have also been caused by the shoaling of the Central

397 American Seaway (Panamanian Seaway) during the middle-late Miocene [*Billups*,
398 2002; *Nisancioglu et al.*, 2003; *Butzin et al.*, 2011].

399 The MOW is predominantly fed by the LIW [*Bryden and Stommel*, 1984].
400 During the Quaternary, cold stadials have been associated with production of a denser
401 LIW [*Cacho et al.*, 2000] that enhanced the current activity and depth of settling of the
402 MOW [*Schönfeld and Zahn*, 2000; *Rogerson et al.*, 2005]. Similarly, during the late
403 Miocene global cooling [*Zachos et al.*, 2001; *Murphy et al.*, 2009] a denser LIW could
404 have enhanced the MOW via increasing its buoyancy loss, which is consistent with the
405 observed increase of the NADW formation and AMOC intensification during this time
406 interval.

407 The final closure of the Guadalhorce Corridor might have produced a dramatic
408 reduction of the MOW, which then could only flow through the Rifian Corridors until
409 their final closure at around 6.0 Ma [*Krijgsman et al.*, 1999a]. This led to a diminished
410 NADW production as is recorded between 6.0 and 5.5 Ma in the South Atlantic
411 [*Billups*, 2002]. Concomitantly, the cessation of the MOW increased the freshwater
412 input in the North Atlantic reducing or interrupting the NADW formation [*Rahmstorf*,
413 1998]. This might have had a critical impact on the AMOC, global thermohaline
414 circulation and global climate [*Bethoux et al.*, 1999]. Specifically, the reduction or
415 interruption of the NADW by MOW cessation would reduce the AMOC leading to
416 northern hemisphere cooling [*Clark et al.*, 2002]. This is supported by development of
417 northern hemisphere ice sheets in Greenland margin [*Fronval and Jansen*, 1996; *Thiede*
418 *et al.*, 1998].

419 Finally, with the restoration of the Atlantic-Mediterranean connections through
420 the Strait of Gibraltar, the MOW enhanced the NADW formation as it is indicated by

421 the rise in NADW flow around the Miocene-Pliocene boundary in the South Atlantic
422 and the western equatorial Atlantic Ocean [King *et al.*, 1997; Billups, 2002].

423

424 **7. Conclusions**

425 The Messinian stable isotope records from the Montemayor-1 core located in the
426 lower Guadalquivir Basin (SW Spain) allow the accurate dating of the closure of the
427 Guadalhorce Corridor, the last Betic Corridor connecting the Atlantic and the
428 Mediterranean before the MSC, at 6.18 Ma.

429 Before the closure of the Guadalhorce Corridor, the export of highly saline
430 intermediate waters as MOW contributed to increased NADW formation in the North
431 Atlantic Ocean. During this period, constant benthic $\delta^{18}\text{O}$ values that depart from the
432 global glacioeustatic trend, high $\Delta\delta^{18}\text{O}_{\text{b-p}}$, and low sedimentation rates indicate a strong
433 water stratification and bottom water winnowing due to the MOW flow. After the
434 closure of the corridor, benthic $\delta^{18}\text{O}$ values, which parallel that of the global
435 glacioeustatic curve, low $\Delta\delta^{18}\text{O}_{\text{b-p}}$, and high sedimentation rates suggest an improved
436 vertical mixing of the water column and interruption of MOW. Changes in the stable O
437 isotope composition of the subsurface North Atlantic water masses during this time
438 interval are primarily controlled by glacioeustatic processes. The cessation of the MOW
439 might have resulted in decreased NADW formation between 6.0 and 5.5 Ma weakening
440 the AMOC and promoting northern hemisphere cooling. Then, the restoration of the
441 MOW due to the opening of the Strait of Gibraltar around the Miocene-Pliocene
442 boundary would have favored an enhanced NADW formation.

443

444 **Acknowledgments**

445 We acknowledge the comments provided by reviewers Michael Rogerson and
446 Marit-Solveig Seidenkrantz which substantially improved the quality of an earlier
447 version of the manuscript. This paper is part of the Research Projects CGL2010-20857
448 and CGL2009-11539/BTE of the Ministerio de Ciencia e Innovación of Spain, and the
449 Research Group RNM-190 of the Junta de Andalucía. JNPA has been funded by a
450 research F.P.U. scholarship (ref. AP2007-00345) provided by the Ministerio de
451 Educación of Spain. We are grateful to N. Andersen (Leibniz-Laboratory, Kiel,
452 Germany) for stable isotope analysis. We also thank L. Vidal who provided the stable
453 isotope data of benthic foraminifera from the ODP Site 1085 (SE Atlantic).

454

455 **References**

- 456 Abouchami, W., S.J.G. Galer, and A. Koschinsky (1999), Pb and Nd isotopes in NE
457 Atlantic Fe–Mn crusts: Proxies for trace metal paleosources and paleocean
458 circulation, *Geochim. Cosmochim. Ac.*, 63, 1489–1505,
459 [http://dx.doi.org/10.1016/S0016-7037\(99\)00068-X](http://dx.doi.org/10.1016/S0016-7037(99)00068-X).
- 460 Aguirre, J. (1992), Evolución de las asociaciones fósiles del Plioceno marino de Cabo
461 Roche (Cádiz), *Rev. Esp. Paleontol., Extra*, 3–10.
- 462 Aguirre, J. (1995), Implicaciones paleoambientales y paleogeográficas de dos
463 discontinuidades estratigráficas en los depósitos pliocénicos de Cádiz (SW de
464 España), *Rev. Soc. Geol. España*, 8, 161–174.
- 465 Aguirre, J., J.C. Braga, and J.M. Martín (1993), Algal nodules in the Upper Pliocene
466 deposits at the coast of Cadiz (S Spain), *Boll. Soc. Paleontol. Ital., Spec. Vol. 1*, 1–7.
- 467 Aguirre, J., C. Castillo, F.J. Ferriz; J. Agustí, and O. Oms (1995), Marine-continental
468 magnetobiostratigraphic correlation of the Dolomys subzone (middle of Late

469 Ruscinian): implications for the Late Ruscinian age, *Palaeogeogr. Palaeoclimatol.*
470 *Palaeoecol.*, 117, 139–152, [http://dx.doi.org/10.1016/0031-0182\(94\)00123-P](http://dx.doi.org/10.1016/0031-0182(94)00123-P).

471 Aguirre, J., J.C. Braga, and J.M. Martín (2007), El Mioceno marino del Prebético
472 occidental (Cordillera Bética, SE de España): historia del cierre del Estrecho
473 Norbético, in: *XIII Jornadas de la Sociedad Española de Paleontología: Guía de*
474 *Excursiones*, edited by J. Aguirre et al., pp. 53–66, Instituto Geológico y Minero de
475 España-Universidad de Granada, Granada.

476 Benson, R.H., K. Rakic-El Bied, and G. Bonaduce (1991), An important current
477 reversal (influx) in the Rifian corridor (Morocco) at the Tortonian-Messinian
478 Boundary: the end of Tethys ocean, *Paleoceanography*, 6, 165–192,
479 doi:10.1029/90PA00756.

480 Bethoux, J. P., B. Gentili, P. Morin, E. Nicolas, C. Pierre, and D. Ruiz - Pino (1999),
481 The Mediterranean Sea: A miniature ocean for climatic and environmental studies
482 and a key for the climatic functioning of the North Atlantic, *Prog. Oceanogr.*, 44,
483 131–146, [http://dx.doi.org/10.1016/S0079-6611\(99\)00023-3](http://dx.doi.org/10.1016/S0079-6611(99)00023-3).

484 Betzler, C., J.C. Braga, J.M. Martín, I.M. Sánchez-Almazo, and S. Lindhorst (2006),
485 Closure of a seaway: Stratigraphic record and facies (Guadix basin, southern Spain),
486 *Int. J. Earth Sci.*, 95, 903–910, doi:10.1007/s00531-006-0073-y.

487 Bigg, G.R., and M.R. Wadley (2001), Millennial-scale variability in the oceans: an
488 ocean modelling view, *J. Quaternary Sci.*, 16, 309–319, doi: 10.1002/jqs.599.

489 Bigg, G.R., T.D. Jickells, P.S. Liss, and T.J. Osborn (2003), The role of the oceans in
490 climate, *Int. J. Climatol.*, 23, 1127–1159, doi: 10.1002/joc.926.

491 Billups, K., (2002), Late Miocene through early Pliocene deep water circulation and
492 climate change viewed from the sub-Antarctic South Atlantic, *Palaeogeogr.*

493 *Palaeoclimatol. Palaeoecol.*, 185, 287–307, <http://dx.doi.org/10.1016/S0031->
494 0182(02)00340-1.

495 Braga, J.C., J.M. Martín, and J. Aguirre (2002), Tertiary. Southern Spain, in *The*
496 *Geology of Spain*, edited by W. Gibbons and T. Moreno, pp 320–327, The
497 Geological Society, London.

498 Braga, J.C., J.M. Martín, and C. Quesada (2003), Patterns and average rates of late
499 Neogene-Recent uplift of the Betic Cordillera, SE Spain, *Geomorphology*, 50, 3–26,
500 [http://dx.doi.org/10.1016/S0169-555X\(02\)00205-2](http://dx.doi.org/10.1016/S0169-555X(02)00205-2).

501 Braga, J.C., J.M. Martín, R. Riding, J. Aguirre, I.M. Sánchez-Almazo, and J. Dinarès-
502 Turell (2006), Testing models for the Messinian salinity crisis: The Messinian record
503 in Almería, SE Spain, *Sediment. Geol.*, 188–189, 131–154,
504 <http://dx.doi.org/10.1016/j.sedgeo.2006.03.002>.

505 Braga, J.C., J.M. Martín, J. Aguirre, C.D. Baird, I. Grunnaleite, N.B. Jensen, A. Puga-
506 Bernabéu, G. Saalen, and M.R. Talbot (2010), Middle-Miocene (Serravallian)
507 temperate carbonates in a seaway connecting the Atlantic Ocean and the
508 Mediterranean Sea (North Betic Strait, S Spain), *Sediment. Geol.*, 225, 19–33,
509 <http://dx.doi.org/10.1016/j.sedgeo.2010.01.003>.

510 Brown, J., A. Colling, D. Park, J. Phillips, D. Rothery, and J. Wright (1989), *Ocean*
511 *Circulation*, The Open University, Pergamon Press, England.

512 Bryden, H.L., and H.M. Stommel (1984), Limiting processes that determine basic
513 features of the circulation in the Mediterranean Sea, *Oceanol. Acta*, 7, 289–296.

514 Butzin, M., G. Lohmann, and T. Bickert (2011), Miocene ocean circulation inferred
515 from marine carbon cycle modeling combined with benthic isotope records,
516 *Paleoceanography*, 26, PA1203, doi:10.1029/2009PA001901.

517 Cacho, I., J.O. Grimalt, F.J. Sierro, N. Shackleton, and M. Canals (2000), Evidence for
518 enhanced Mediterranean thermohaline circulation during rapid climatic coolings,
519 *Earth Planet. Sc. Lett.*, 183, 417–429, [http://dx.doi.org/10.1016-](http://dx.doi.org/10.1016/S0012-821X(00)00296-X)
520 821X(00)00296-X.

521 Clark, P. U., N. G. Pisias, T. F. Stocker, and A. J. Weaver (2002), The role of the
522 thermohaline circulation in abrupt climate change, *Nature*, 415, 863–869,
523 doi:10.1038/415863a

524 Esteban, M., J.C. Braga, J.M. Martín, and C. Santisteban (1996), Western
525 Mediterranean reef complexes, in: *Models for Carbonate Stratigraphy from Miocene*
526 *Reef Complexes of Mediterranean Regions. Concepts in Sedimentology and*
527 *Paleontology*, vol. 5., edited by E.K. Franseen et al., pp. 55–72, Society of Economic
528 Paleontologists and Mineralogists, Tulsa, Oklahoma.

529 Estrada, F., G. Ercilla, C. Gorini, B. Alonso, J.T. Vázquez, D. García-Castellanos, C.
530 Juan, A. Maldonado, A. Ammar, and M. Elabbassi (2011), Impact of pulsed Atlantic
531 water inflow into the Alboran Basin at the time of the Zanclean flooding, *Geo-Mar.*
532 *Lett.*, 31, 361-376, DOI: 10.1007/s00367-011-0249-8.

533 Fronval, T. and Jansen, E. (1996) Late Neogene paleoclimates and paleoceanography in
534 the Iceland-Norwegian Sea: evidence from the Iceland and Vøring Plateaus. *Proc.*
535 *Ocean Drill. Program Sci. Results*, 151, 455–468,
536 doi:10.2973/odp.proc.sr.151.134.1996.

537 Garcés, M., W. Krijgsman, and J. Agustí (1998), Chronology of the late Turolian
538 deposits of the Fortuna basin (SE Spain): implications for the Messinian evolution of
539 the eastern Betics, *Earth Planet. Sc. Lett.*, 163, 69–81,
540 [http://dx.doi.org/10.1016/S0012-821X\(98\)00176-9](http://dx.doi.org/10.1016/S0012-821X(98)00176-9).

541 González-Delgado, J.A., J. Civis, C.J. Dabrio, J.L. Goy, S. Ledesma, J. Pais, F.J. Sierro,
542 and C. Zazo (2004), Cuenca del Guadalquivir, in *Geología de España*, edited by J.A.
543 Vera, pp. 543–550, SGE-IGME, Madrid.

544 Hammer, Ø., D.A.T. Harper, and P. D. Ryan (2001), PAST: Paleontological Statistics
545 Software Package for Education and Data Analysis, *Palaeontol. Elec.*, *4*, 1–9.

546 Hernández-Molina, F.J., E. Llave, D.A.V. Stow, M. García, L. Somoza, J.T. Vázquez,
547 F.J. Lobo, A. Maestro, B. Díaz del Río, R. León, T. Medialdea, and J. Gardner
548 (2006), The contourite depositional system of the Gulf of Cádiz: A sedimentary
549 model related to the bottom current activity of the Mediterranean outflow water and
550 its interaction with the continental margin, *Deep-Sea Res. Pt. II*, *53*, 1420–1463,
551 <http://dx.doi.org/10.1016/j.dsr2.2006.04.016>.

552 Hernández-Molina F.J., N. Serra, D.A.V. Stow, E. Llave, G. Ercilla, and D. Van Rooij
553 (2011), Along-slope oceanographic processes and sedimentary products around the
554 Iberian margin, *Geo-Mar. Lett.*, *31*, 315–341, DOI: 10.1007/s00367-011-0242-2.

555 Hodell, D.A., R.H. Benson, D.V. Kent, A. Boersma, and K. Rakic-El Bied (1994),
556 Magnetostratigraphic, biostratigraphic, and stable isotope stratigraphy of an Upper
557 Miocene drill core from the Salé Briqueterie (northwestern Morocco): A high-
558 resolution chronology for the Messinian stage, *Paleoceanography*, *9*, 835–855,
559 doi:10.1029/94PA01838.

560 Hodell, D.A., J.H. Curtis, F.J. Sierro, and M.E. Raymo (2001), Correlation of late
561 Miocene to early Pliocene sequences between the Mediterranean and North Atlantic,
562 *Paleoceanography*, *16*, 164–178, doi:10.1029/1999PA000487.

563 Hsü, K.J., W.B.F. Ryan, and M.B. Cita (1973), Late Miocene Desiccation of the
564 Mediterranean, *Nature*, *242*, 240–244, doi:10.1038/242240a0.

565 Hsü, J.K., L. Montadert, D. Bernoulli, M.B. Cita, A. Erickson, R.E. Garrison, R.B.
566 Kidd, F. Mélières, C. Müller, and R. Wright (1977), History of the Mediterranean
567 salinity crisis, *Nature*, 267, 1053–1078, doi:10.1038/267399a0.

568 Huang, T.C. and D.J. Stanley (1972), Western Alboran Sea: sediment dispersal,
569 ponding and reversal of currents, in: *The Mediterranean Sea: a natural*
570 *sedimentation laboratory*, edited by D.J. Stanley et al., pp. 521–559, Dowden,
571 Hutchinson & Ross, Stroudsburg.

572 Keigwin, L.D., M.P. Aubry, and D.V. Kent (1987), North Atlantic late Miocene stable-
573 isotope stratigraphy, biostratigraphy, and magnetostratigraphy, *Initial Reports of the*
574 *DSDP, 94*, 935-963.

575 Khélifi, N., M. Sarnthein, N. Andersen, T. Blanz, M. Frank, D. Garbe-Schönberg, B.A.
576 Haley, R. Stumpf, and M. Weinelt (2009), A major and long-term Pliocene
577 intensification of the Mediterranean outflow, 3.5-3.3 Ma ago, *Geology*, 37, 811–814,
578 doi:10.1130/G30058A.1.

579 King, T. A., W. G. Ellis Jr., D. W. Murray, N. J. Shackleton, and S. Harris (1997),
580 Miocene evolution of carbonate sedimentation at the Ceara rise: A multivariate
581 data/proxy approach, in *Proc. Ocean Drill. Program Sci. Results*, edited by N. J.
582 Shackleton et al., pp. 349–365, Ocean Drill. Program, College Station, Tex..

583 Krijgsman, W., C.G. Langereis, W.J. Zachariasse, M. Boccaletti, G. Moratti, R. Gelati,
584 S. Iaccarino, G. Papani, and G. Villa (1999a), Late Neogene evolution of the Taza-
585 Guercif Basin (Rifian Corridor, Morocco) and implications for the Messinian salinity
586 crisis, *Mar. Geol.*, 153, 147–160, [http://dx.doi.org/10.1016/S0025-3227\(98\)00084-](http://dx.doi.org/10.1016/S0025-3227(98)00084-)
587 X.

588 Krijgsman, W., F.J. Hilgen, I. Raffi, F.J. Sierro, and D.S. Wilson (1999b), Chronology,
589 causes and progression of the Messinian salinity crisis, *Nature*, *400*, 652–655,
590 doi:10.1038/23231.

591 Krijgsman, W., S. Gaboardi, F.J. Hilgen, S. Iaccarino, E. de Kaenel, and E. van der
592 Laan, (2004), Revised astrochronology for the Ain el Beida section (Atlantic
593 Morocco): No glacio-eustatic control for the onset of the Messinian Salinity Crisis,
594 *Stratigraphy*, *1*, 87–101.

595 Lacombe, H., P. Tchernia, and L. Gamberoni (1985), Variable bottom water in the
596 western Mediterranean basin, *Prog. Oceanogr.*, *14*, 319–338,
597 [http://dx.doi.org/10.1016/0079-6611\(85\)90015-1](http://dx.doi.org/10.1016/0079-6611(85)90015-1).

598 Larrasoana, J.C., J.A. González-Delgado, J. Civis, F.J. Sierro, G. Alonso-Gavilán, and
599 J. Pais (2008), Magnetobiostratigraphic dating and environmental magnetism of Late
600 Neogene marine sediments recovered at the Huelva-1 and Montemayor-1 boreholes
601 (lower Guadalquivir basin, Spain), *Geo-Temas*, *10*, 1175–1178.

602 Llave, E., J. Schönfeld, F.J. Hernández-Molina, T. Mulder, L. Somoza, V. Díaz del Río,
603 and I. Sánchez-Almazo (2006), High-resolution stratigraphy of the Mediterranean
604 outflow contourite system in the Gulf of Cadiz during the late Pleistocene: The
605 impact of Heinrich events, *Mar. Geol.*, *227*, 241–262,
606 <http://dx.doi.org/10.1016/j.margeo.2005.11.015>.

607 Llave, E., H. Matías, F.J. Hernández-Molina, G. Ercilla, D.A.V. Stow, and T.
608 Medialdea (2011), Pliocene-Quaternary contourites along the northern Gulf of Cadiz
609 margin: sedimentary stacking pattern and regional distribution, *Geo-Mar. Lett.*, *31*,
610 377-390, DOI: 10.1007/s00367-011-0241-3.

611 Loubere, P. (1987) Changes in mid-depth North Atlantic and Mediterranean circulation
612 during the late Pliocene—Isotopic and sedimentological evidence, *Mar. Geol.*, 77,
613 15–38, [http://dx.doi.org/10.1016/0025-3227\(87\)90081-8](http://dx.doi.org/10.1016/0025-3227(87)90081-8).

614 Lourens, L.J., F.J. Hilgen, N.J. Shackleton, J. Laskar, and D.S. Wilson (2004), The
615 Neogene Period, in *A Geologic Time Scale 2004*, edited by F.M. Gradstein et al., pp.
616 409–440, Cambridge University Press, Cambridge.

617 Maldonado, A., and C.H. Nelson (1999), Interaction of tectonic and depositional
618 processes that control the evolution of the Iberian Gulf of Cadiz margin, *Mar. Geol.*,
619 155, 217–242, [http://dx.doi.org/10.1016/S0025-3227\(98\)00148-0](http://dx.doi.org/10.1016/S0025-3227(98)00148-0).

620 Marshall, J., and F. Schott (1999), Open-ocean convection: Observations, theory, and
621 models, *Rev. Geophys.*, 37, 1–64, doi: 10.1029/98RG02739.

622 Martín, J.M., J.C. Braga, and C. Betzler (2001), The Messinian Guadalhorce Corridor:
623 the last northern, Atlantic-Mediterranean gateway, *Terra Nova*, 13, 418–424,
624 doi:10.1046/j.1365-3121.2001.00376.x.

625 Martín, J.M., J.C. Braga, J. Aguirre, and A. Puga-Bernabéu (2009), History and
626 evolution of the North-Betic Strait (Prebetic Zone, Betic Cordillera): A narrow, early
627 Tortonian, tidal-dominated, Atlantic-Mediterranean marine passage, *Sediment. Geol.*,
628 216, 80–90, <http://dx.doi.org/10.1016/j.sedgeo.2009.01.005>.

629 MEDOC Group (1970), Observation of formation of deep water in the Mediterranean
630 Sea, *Nature*, 227, 1037–1040, doi:10.1038/2271037a0.

631 Millot, C. (1999), Circulation in the western Mediterranean Sea, *J. Mar. Syst.*, 20, 423–
632 442, doi:10.1016/S0924-7963(98)00078-5.

633 Murphy, L.N., D.B. Kirk-Davidoff, N. Mahowald, and B.L. Otto-Bliesner (2009), A
634 numerical study of the climate response to lowered Mediterranean Sea level during

635 the Messinian Salinity Crisis, *Palaeogeogr. Palaeoclimatol. Palaeoecol.*, 279,
636 41–59, <http://dx.doi.org/10.1016/j.palaeo.2009.04.016>.

637 Nelson, C.H. (1990), Estimated post-Messinian sediment supply and sedimentation
638 rates on the Ebro continental margin, Spain, *Mar. Geol.*, 95, 395–418.
639 [http://dx.doi.org/10.1016/0025-3227\(90\)90126-5](http://dx.doi.org/10.1016/0025-3227(90)90126-5).

640 Nelson, C.H., J. Baraza, and A. Maldonado (1993), Mediterranean undercurrent sandy
641 contourites, Gulf of Cádiz, Spain, *Sediment. Geol.*, 82, 103–131,
642 [http://dx.doi.org/10.1016/0037-0738\(93\)90116-M](http://dx.doi.org/10.1016/0037-0738(93)90116-M).

643 Nisancioglu, K., M. E. Raymo, and P. H. Stone (2003), Reorganization of Miocene
644 deep water circulation in response to the shoaling of the Central American Seaway,
645 *Paleoceanography*, 18, 1006, doi: 10.102912002PA000767.

646 Pérez-Asensio, J.N., J. Aguirre, G. Schmiedl, and J. Civis (2012), Messinian
647 paleoenvironmental evolution in the lower Guadalquivir Basin (SW Spain) based on
648 benthic foraminifera, *Palaeogeogr., Palaeoclimatol., Palaeoecol.*, 326-328,
649 135–151, <http://dx.doi.org/10.1016/j.palaeo.2012.02.014>.

650 Pinardi, N., and E. Masetti, (2000), Variability of the large scale general circulation of
651 the Mediterranean Sea from observations and modelling: a review, *Palaeogeogr.*
652 *Palaeoclimatol. Palaeoecol.*, 158, 153–173, [http://dx.doi.org/10.1016/S0031-](http://dx.doi.org/10.1016/S0031-0182(00)00048-1)
653 [0182\(00\)00048-1](http://dx.doi.org/10.1016/S0031-0182(00)00048-1).

654 Price, J. F., and M. O'Neill-Baringer (1994), Outflows and deep water production by
655 marginal seas, *Prog. Oceanogr.*, 33, 161–200, doi:10.1016/0079-6611(94)90027-2.

656 Raddatz, J., A. Rüggeberg, S. Margreth, W.-C., Dullo, and IODP Expedition 307
657 Scientific Party (2011), Paleoenvironmental reconstruction of Challenger Mound
658 initiation in the Porcupine Seabight, NE Atlantic, *Mar. Geol.*, 282, 79–90,
659 <http://dx.doi.org/10.1016/j.margeo.2010.10.019>.

660 Rahmstorf, S. (1998), Influence of Mediterranean Outflow on climate, *Eos Trans. AGU*,
661 79, 281–282.

662 Reid, J.L. (1979), On the contribution of the Mediterranean Sea outflow to the
663 Norwegian-Greenland Sea, *Deep-Sea Res.*, 26, 1199–1223,
664 [http://dx.doi.org/10.1016/0198-0149\(79\)90064-5](http://dx.doi.org/10.1016/0198-0149(79)90064-5).

665 Riaza, C., and W. Martínez del Olmo (1996), Depositional model of the Guadalquivir-
666 Gulf of Cádiz Tertiary basin, in *Tertiary basins of Spain*, edited by P. Friend and C.J.
667 Dabrio, pp. 330–338, Cambridge University Press, Cambridge.

668 Riding, R., J. C. Braga, J. M. Martin, and I. M. Sánchez-Almazo (1998), Mediterranean
669 Messinian salinity crisis: Constraints from a coeval marginal basin, Sorbas, SE
670 Spain, *Mar. Geol.*, 146, 1-20, [http://dx.doi.org/10.1016/S0025-3227\(97\)00136-9](http://dx.doi.org/10.1016/S0025-3227(97)00136-9).

671 Rogerson, M., E.J. Rohling, P.P.E. Weaver, and J.W. Murray (2005), Glacial to
672 interglacial changes in the settling depth of the Mediterranean Outflow plume,
673 *Paleoceanography*, 20, PA3007, doi:10.1029/2004PA001106.

674 Rogerson, M., E.J. Rohling, and P.P.E. Weaver (2006), Promotion of meridional
675 overturning by Mediterranean-derived salt during the last deglaciation.
676 *Paleoceanography*, 21, PA4101 doi:10.1029/2006PA001306.

677 Rogerson, M., E. Colmenero-Hidalgo, R.C Levine, L. de Abreu, E. J. Rohling, A.H.L.
678 Voelker, G.R. Bigg, J. Schönfeld, I. Cacho, F.J. Sierro, L. Löwemark, M.I. Reguera,
679 M.I., L. de Abreu, and K. Garrick, (2010), Enhanced Mediterranean-Atlantic
680 exchange during Atlantic freshening phases, *Geochem. Geophys. Geosyst.*, 11,
681 Q08013, doi:10.1029/2009GC002931.

682 Rogerson, M., J. Schönfeld, and M.J. Leng (2011), Qualitative and quantitative
683 approaches in palaeohydrography: A case study from core-top parameters in the Gulf
684 of Cadiz, *Mar. Geol.*, 280, 150–167, doi:10.1016/j.margeo.2010.12.008.

685 Rogerson, M., E. J. Rohling, G. R. Bigg, and J. Ramirez (2012), Paleocyanography of
686 the Atlantic-Mediterranean exchange: Overview and first quantitative assessment of
687 climatic forcing, *Rev. Geophys.*, *50*, RG2003, doi:10.1029/2011RG000376.

688 Sanz de Galdeano, C., and J.A. Vera (1992), Stratigraphic record and
689 palaeogeographical context of the Neogene basins in the Betic Cordillera, Spain,
690 *Basin Res.*, *4*, 21–36, doi: 10.1111/j.1365-2117.1992.tb00040.x.

691 Sanz de Galdeano C. and J. Rodríguez-Fernández (1996), Neogene palaeogeography of
692 the Betic Cordillera: an attempt at reconstruction, in *Tertiary basins of Spain*, edited
693 by P. Friend and C.J. Dabrio, pp. 323–329, Cambridge University Press, Cambridge.

694 Schönfeld, J. (1997), The impact of the Mediterranean Outflow Water (MOW) on
695 benthic foraminiferal assemblages and surface sediments at the southern Portuguese
696 continental margin, *Mar. Micropaleontol.*, *29*, 211–236,
697 [http://dx.doi.org/10.1016/S0377-8398\(96\)00050-3](http://dx.doi.org/10.1016/S0377-8398(96)00050-3).

698 Schönfeld, J., and R. Zahn (2000), Late Glacial to Holocene history of the
699 Mediterranean Outflow. Evidence from benthic foraminiferal assemblages and stable
700 isotopes at the Portuguese margin, *Palaeogeogr. Palaeoclimatol. Palaeoecol.*, *159*,
701 85–111, [http://dx.doi.org/10.1016/S0031-0182\(00\)00035-3](http://dx.doi.org/10.1016/S0031-0182(00)00035-3).

702 Schulz, M., and M. Mudelsee (2002), REDFIT: estimating red-noise spectra directly
703 from unevenly spaced paleoclimatic time series, *Comput. Geosci.*, *28*, 421–426,
704 [http://dx.doi.org/10.1016/S0098-3004\(01\)00044-9](http://dx.doi.org/10.1016/S0098-3004(01)00044-9).

705 Shackleton, N.J., M.A. Hall, and D. Pate (1995), Pliocene stable isotope stratigraphy of
706 site 846, *Proc. Ocean Drill. Program Sci. Results*, *138*, 337–355,
707 doi:10.2973/odp.proc.sr.138.117.1995.

708 Sierro, F.J., J.A. Flores, J. Civis, J. A. González-Delgado, and G. Francés (1993), Late
709 Miocene globorotaliid event-stratigraphy and biogeography in the NE-Atlantic and

710 Mediterranean, *Mar. Micropaleontol.*, 21, 143–167, <http://dx.doi.org/10.1016/0377->
711 8398(93)90013-N.

712 Sierro, F.J., J.A. González-Delgado, C.J. Dabrio, J.A. Flores, and J. Civis (1996), Late
713 Neogene depositional sequences in the foreland basin of Guadalquivir (SW Spain),
714 in *Tertiary basins of Spain*, edited by P. Friend and C.J. Dabrio, pp. 339–345,
715 Cambridge University Press, Cambridge.

716 Sierro, F.J., D.A. Hodell, J.H. Curtis, J.A. Flores, I. Reguera, E. Colmenero-Hidalgo,
717 M.A. Bárcena, J.O. Grimalt, I. Cacho, J. Frigola, and M. Canals (2005), Impact of
718 iceberg melting on Mediterranean thermohaline circulation during Heinrich events,
719 *Paleoceanography*, 20, PA2019, doi:10.1029/2004PA001051.

720 Stumpf, R., M. Frank, J. Schönfeld, and B.A. Haley (2010), Late Quaternary variability
721 of Mediterranean Outflow Water from radiogenic Nd and Pb isotopes, *Quaternary*
722 *Sci. Rev.*, 29, 2462–2472, doi:10.1016/j.quascirev.2010.06.021.
723 <http://dx.doi.org/10.1016/j.quascirev.2010.06.021>.

724 Thiede, J., A. Winkler, T. Wolf-Welling, O. Eldholm, A. M. Myhre, K.-H. Baumann, R.
725 Henrich, and R. Stein (1998), Late Cenozoic history of the polar North Atlantic:
726 Results from ocean drilling, *Quat. Sci. Rev.*, 17, 185 – 208, doi:10.1016/S0277-
727 3791(97)00076-0.

728 Toucanne, S., T. Mulder, J. Schönfeld, V. Hanquiez, E. Gonthier, J. Duprat, M. Cremer,
729 and S. Zaragosi (2007), Contourites of the Gulf of Cadiz: a high-resolution record of
730 the paleocirculation of the Mediterranean Outflow Water during the last 50,000
731 years, *Palaeogeogr. Palaeoclimatol. Palaeoecol.*, 246, 354–366,
732 <http://dx.doi.org/10.1016/j.palaeo.2006.10.007>.

733 Van der Laan, E., S. Gaboardi, F.J. Hilgen, and L.J. Lourens (2005), Regional climate
734 and glacial control on high-resolution oxygen isotope records from Ain El Beida

735 (latest Miocene, northwest Morocco): A cyclostratigraphic analysis in the depth and
736 time domain, *Paleoceanography*, 20, PA1001, doi: 10.1029/2003PA000995.

737 Van der Laan, E., F.J. Hilgen, L.J. Lourens, E. de Kaenel, S. Gaboardi, and S. Iaccarino
738 (2012), Astronomical forcing of Northwest African climate and glacial history during
739 the late Messinian (6.5-5.5 Ma), *Palaeogeogr. Palaeoclimatol. Palaeoecol.*, 313-314
740 107–126, <http://dx.doi.org/10.1016/j.palaeo.2011.10.013>.

741 Van Rooij, D., J. Iglesias, F.J. Hernández-Molina, G. Ercilla, M. Gomez-Ballesteros, D.
742 Casas, E. Llave, A. De Hauwere, S. Garcia-Gil, J. Acosta, and J.-P. Henriot (2010),
743 The Le Danois Contourite Depositional System: Interactions between the
744 Mediterranean Outflow Water and the upper Cantabrian slope (North Iberian
745 margin), *Mar. Geol.*, 274, 1–20, <http://dx.doi.org/10.1016/j.margeo.2010.03.001>.

746 Vera, J.A. (2000), El Terciario de la Cordillera Bética: estado actual de conocimientos,
747 *Rev. Soc. Geol. España*, 13, 345–373.

748 Vergnaud-Grazzini, C. (1983), Reconstruction of Mediterranean Late Cenozoic
749 hydrography by means of carbon isotope analyses, *Utrecht Micropaleontol Bull.*, 30,
750 25–47.

751 Vidal, L., T. Bickert, G. Wefer, and U. Röhl (2002), Late Miocene stable isotope
752 stratigraphy of SE Atlantic ODP Site 1085: Relation to Messinian events, *Mar.*
753 *Geol.*, 180, 71–85, [http://dx.doi.org/10.1016/S0025-3227\(01\)00206-7](http://dx.doi.org/10.1016/S0025-3227(01)00206-7).

754 Voelker, A.H.L., S.M. Lebreiro, J. Schönfeld, I. Cacho, H. Erlenkeuser, and F. Abrantes
755 (2006), Mediterranean outflow strengthening during northern hemisphere coolings:
756 A salt source for the glacial Atlantic?, *Earth Planet. Sc. Lett.*, 245, 39–55,
757 <http://dx.doi.org/10.1016/j.epsl.2006.03.014>.

758 Wüst, G. (1961), On the vertical circulation of the Mediterranean Sea, *J. Geophys. Res.*,
759 66, 3261-3271, doi:10.1029/JZ066i010p03261.

760 Zachos, J.C., M. Pagani, L. Sloan, E. Thomas, and K. Billups (2001), Trends, Rhythms,
761 and Aberrations in Global Climate 65 Ma to Present, *Science*, 292, 686–693, DOI:
762 10.1126/science.1059412.

763 Zhang, J., and D.B. Scott (1996), Integrated stratigraphy and paleoceanography of the
764 Messinian (latest Miocene) across the North Atlantic Ocean, *Mar. Micropaleontol.*,
765 29, 1–36, [http://dx.doi.org/10.1016/0377-8398\(96\)00010-2](http://dx.doi.org/10.1016/0377-8398(96)00010-2).

766

767 **Figure captions**

768

769 **Figure 1.** (a) Present salinity and circulation patterns at the Strait of Gibraltar and in the
770 Mediterranean [based on *Wüst*, 1961]. The dense and saline Mediterranean intermediate
771 and deep waters form a bottom outflow, while lower salinity surface waters from the
772 Atlantic enters the Mediterranean representing an anti-estuarine circulation pattern. (b)
773 Present-day general circulation pattern at the eastern North Atlantic and Mediterranean
774 Sea [based on *Hernández-Molina et al.*, 2011; *Pinardi and Masetti*, 2000].
775 Mediterranean Outflow Water (MOW), North Atlantic Deep Water (NADW),
776 Levantine Intermediate Water (LIW), Western Mediterranean Deep Water (WMDW)
777 and WMDW formation are indicated.

778

779 **Figure 2.** Geological setting of the lower Guadalquivir Basin. Asterisk indicates the
780 location of the Montemayor-1 core.

781

782 **Figure 3.** Age model, estimation of the sedimentation rate (estimated in cm/kyr) and
783 magnetobiostratigraphic framework for the Montemayor-1 core. Magnetostratigraphy is
784 based on the ATNTS2004 [*Lourens et al.*, 2004]. Type 1 samples have higher quality
785 than types 2 & 3 samples. CrRM is the characteristic remanent magnetization.
786 Biostratigraphy has been established using the planktonic foraminiferal events (PF
787 events) of *Sierro et al.* [1993] and first occurrence of *Globorotalia puncticulata*.
788 Position of glacial stage TG 22 is indicated. Question marks show uncertainties in the
789 chronology and sedimentation rate.

790

791 **Figure 4.** Benthic (*Cibicidoides pachydermus*) stable oxygen isotope record *versus* core
792 depth (gray line) and three-point running average of the benthic oxygen isotope record
793 (black line) of the Montemayor-1 core. Glacial stages TG 20 and TG 22 defined by
794 *Shackleton et al.* [1995] in benthic oxygen isotope record of the ODP site 846 are
795 indicated.

796

797 **Figure 5.** Benthic (*Cibicidoides pachydermus*) stable oxygen isotope record *versus* time
798 (gray lines) and three-point running average of the benthic oxygen isotope record (black
799 lines) from the Site 1085 [*Vidal et al.*, 2002] and Montemayor-1 core. The obliquity
800 component of the benthic isotope record is extracted by sinusoidal curve fitting with a
801 period of 41 kyr. The onset of the Messinian salinity crisis (MSC) is indicated (vertical
802 gray bar in the lower diagram). The vertical black line at 6.18 Ma marks the end of the
803 Atlantic-Mediterranean connection through the Guadalhorce Corridor. Glacial stages
804 from TG 20 to TG 32 defined by *Shackleton et al.* [1995] and from C3An. $\delta^{18}\text{O}$.2 to
805 C3An. $\delta^{18}\text{O}$.8 according to the nomenclature used in *Hodell et al.* [1994] are indicated.
806 The two vertical black solid lines mark glacial stages TG 20 and 22 from the
807 Montemayor-1 core and Site 1085. Vertical gray dashed lines mark glacial stages and
808 the obliquity component of the benthic oxygen isotope record of the Montemayor-1
809 core.

810

811 **Figure 6.** Power spectrum of the benthic (*Cibicidoides pachydermus*) stable oxygen
812 isotope record of the Montemayor-1 core with main orbital periodicities indicated in
813 kiloyears. The 95% confidence interval (CI) is indicated.

814

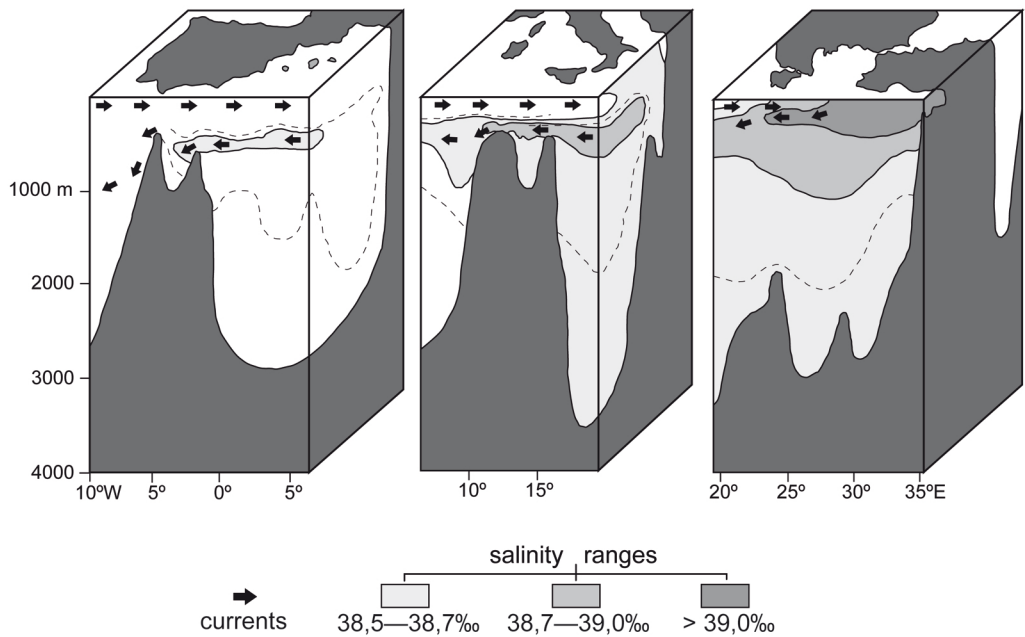
815 **Figure 7.** Benthic (*Cibicidoides pachydermus*) and planktonic (*Globigerina bulloides*)
816 $\delta^{18}\text{O}$ and $\delta^{13}\text{C}$ records in ‰ VPDB, difference between $\delta^{18}\text{O}$ and $\delta^{13}\text{C}$ values of benthic
817 and planktonic foraminifera ($\Delta\delta^{18}\text{O}_{\text{b-p}}$ and $\Delta\delta^{13}\text{C}_{\text{b-p}}$), as well as the planktonic-benthic
818 ratio (P/B ratio) *versus* time (gray lines) and three-point running average (black lines) of
819 the Montemayor-1 core. The vertical dashed line at 6.18 Ma marks the end of the
820 Atlantic-Mediterranean connection through the Guadalhorce Corridor.

821

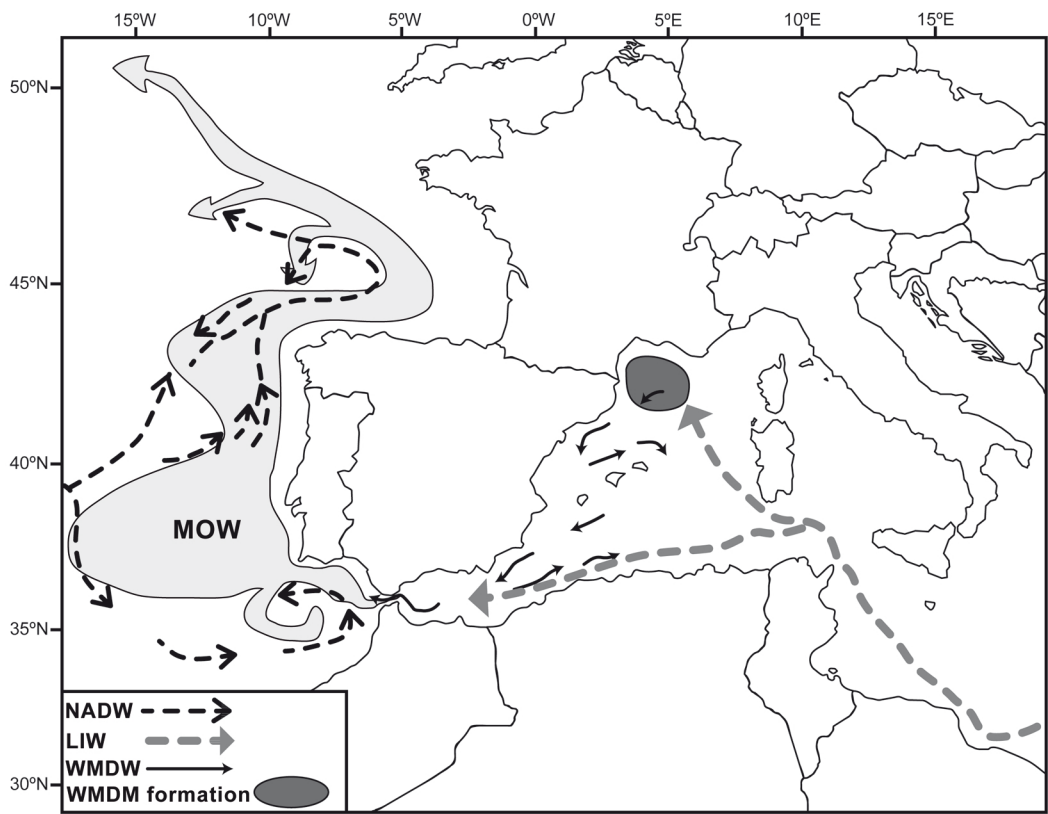
822 **Figure 8.** Paleogeographic and paleoceanographic evolution of the lower Guadalquivir
823 Basin during the Messinian [based on *Martín et al.*, 2009]: a) situation before 6.18 Ma,
824 when the Mediterranean Outflow Water (MOW) reaches the studied core (asterisk); and
825 b) situation after 6.18 Ma, when the MOW was interrupted. The black thick arrow
826 marks the progradation of the main depositional systems along the axis of the
827 Guadalquivir Basin.

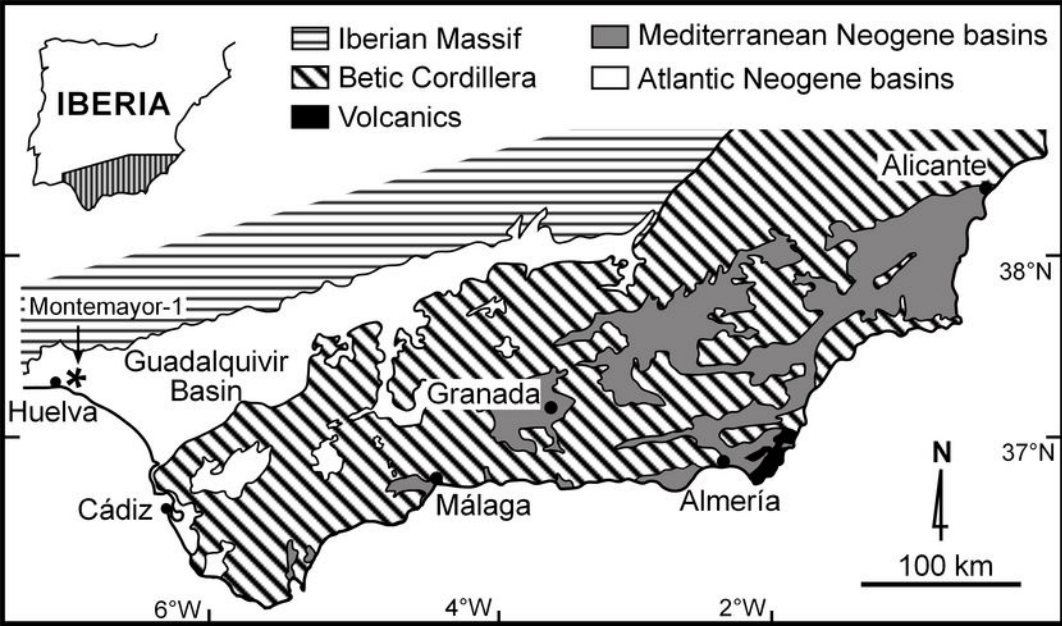
828

a)

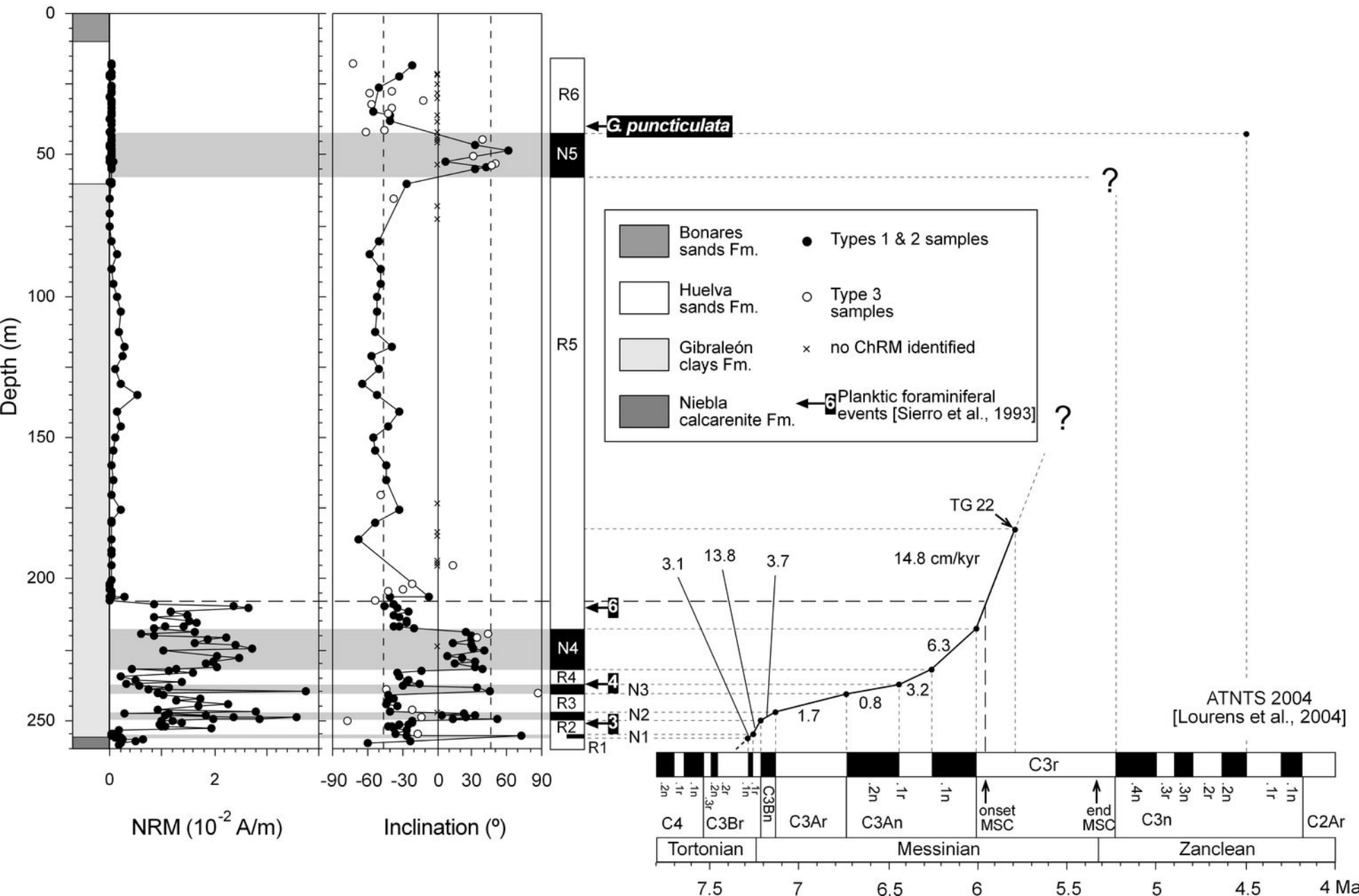


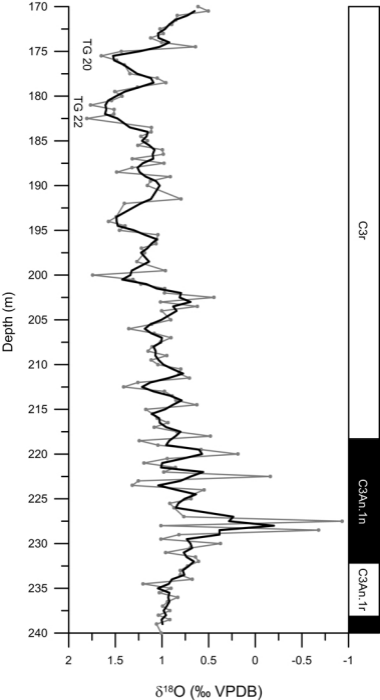
b)

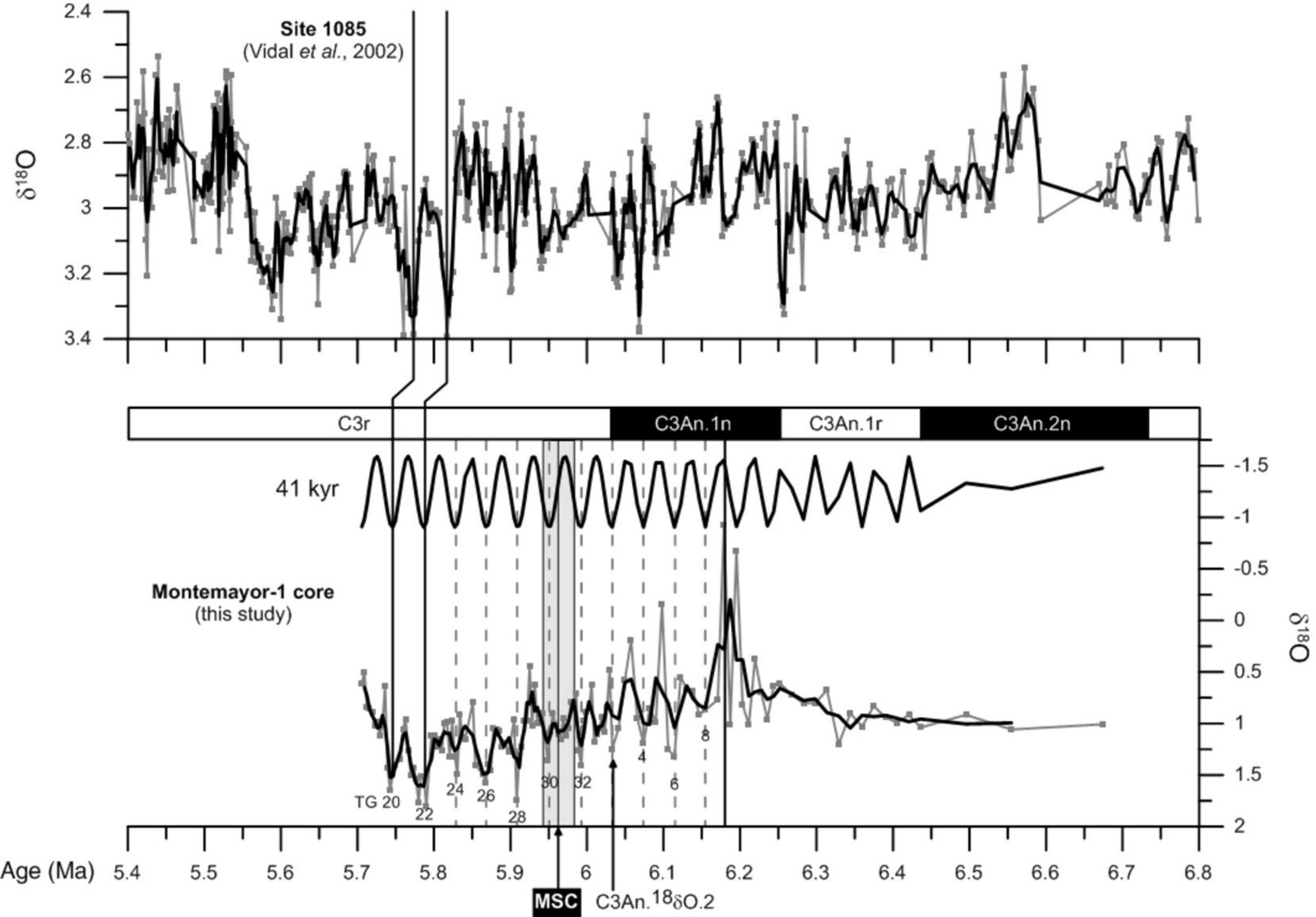




Montemayor-1 core







Cibicoides pachydermus

$\delta^{18}\text{O}$

